

Regularization of Voxel Art

Supplementary material: Additional results and comparisons

David Coeurjolly
CNRS, Université de Lyon

Pierre Gueth
Arskan

Jacques-Olivier Lachaud
Université Savoie Mont-Blanc

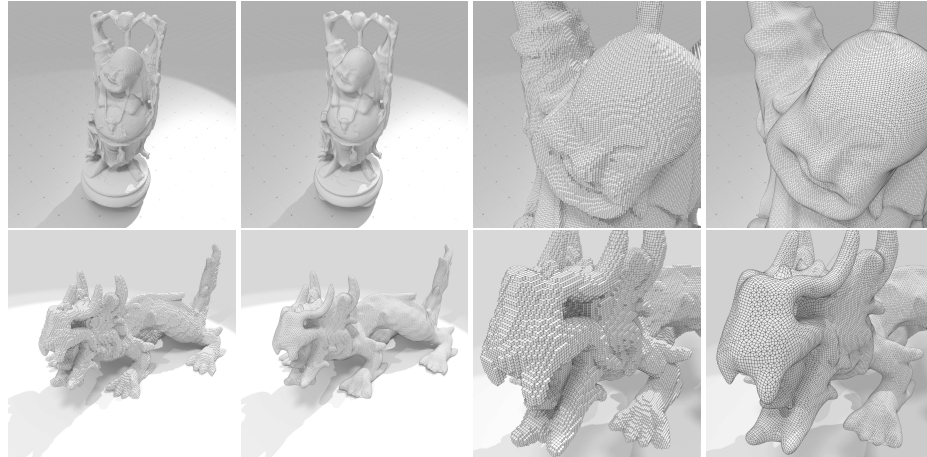


Figure 1: Regularization on higher resolution voxel shapes: Buddha and Dragon in a 256^3 domain.

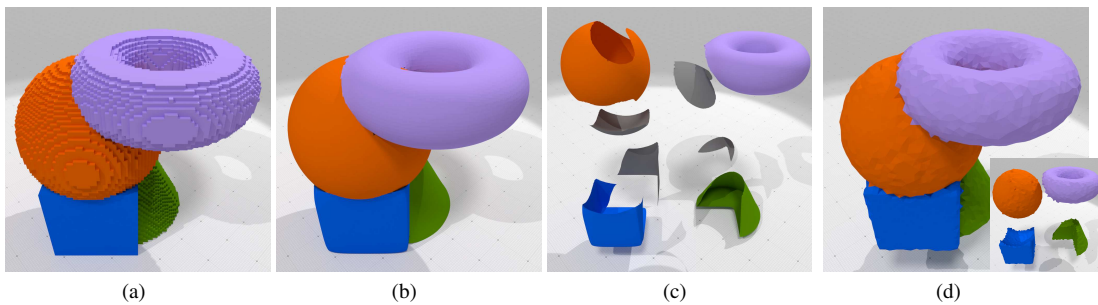


Figure 2: Multi-labeled image with four shapes (75^3) (a). In (b) and (c) the regularization obtained by our approach ($\alpha = 10^{-3}$, $\beta = 1$ and $\gamma = 10^{-1}$). In (d) we have the interfaces obtained using a volumetric tetrahedrization from [AJR⁺17].

References

- Pierre Alliez, Clément Jamin, Laurent Rineau, Stéphane Tayeb, Jane Tournois, and Mariette Yvinec. 3D mesh generation. In *CGAL User and Reference Manual*. CGAL Editorial Board, 4.11 edition, 2017.
- Alexandre Boulch and Renaud Marlet. Fast and robust normal estimation for point clouds with sharp features. *Computer Graphics Forum*, 31(5):1765–1774, 2012.
- David Coeurjolly, Marion Foare, Pierre Gueth, and Jacques-Olivier Lachaud. Piecewise smooth reconstruction of normal vector field on digital data. *Computer Graphics Forum, Pacific Graphics 2016 Proceedings*, 35(7), September 2016.
- David Coeurjolly, Jacques-Olivier Lachaud, and Jérémie Levallois. Multigrid Convergent Principal Curvature Estimators in Digital Geometry. *Computer Vision and Image Understanding*, 129(1):27–41, June 2014.
- Wangyu Zhang, Bailin Deng, Juyong Zhang, Sofien Bouaziz, and Ligang Liu. Guided mesh normal filtering. In *Computer Graphics Forum*, volume 34, pages 23–34. Wiley Online Library, 2015.

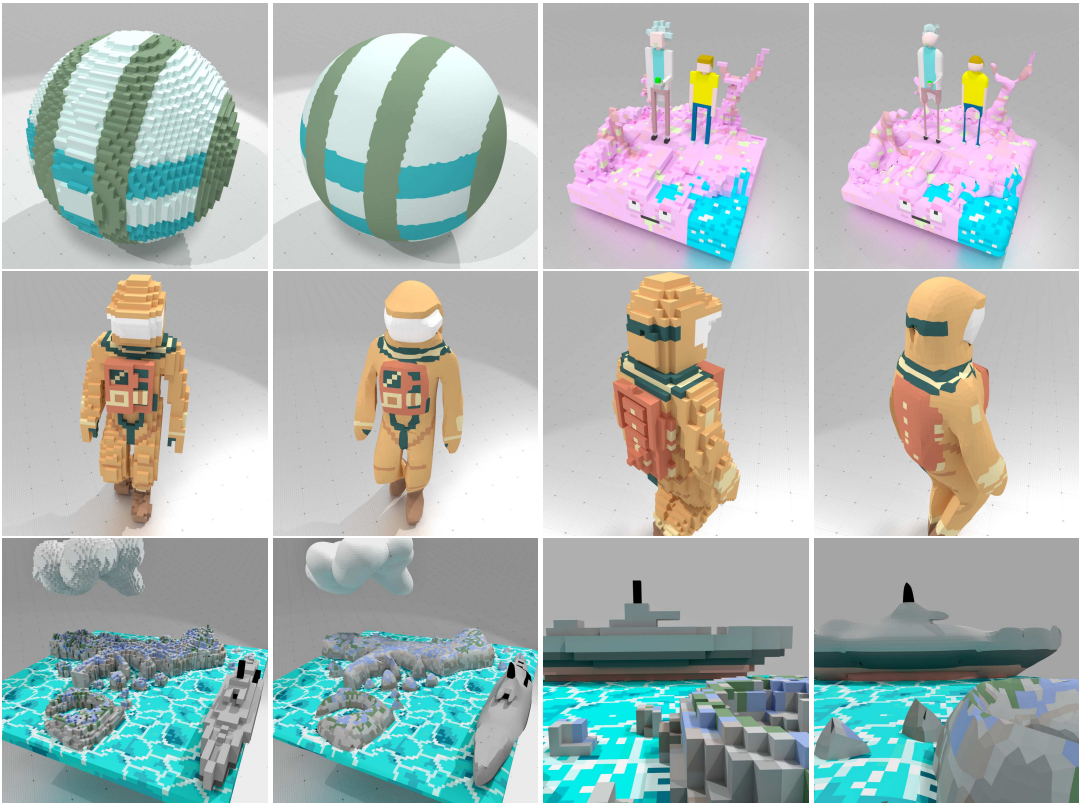


Figure 3: Various voxel art regularization results. First row, a 50^3 ball and a 45^3 voxel scene with very thin structures. Second row: $25 \times 20 \times 65$ volume with 2 regions, one for the helmet glass and one for the rest. Third row: 127^3 volume with four regions: the sea, the ship, the cloud and the island. All experiments have been obtained with the same parameters ($\alpha = 10^{-3}$, $\beta = 1$ and $\gamma = 10^{-1}$). Voxel artwork courtesy of Elbriga (https://twitter.com/gabriel_d_L) and Mike Judge (<https://github.com/mikelovesrobots/mmmm>).

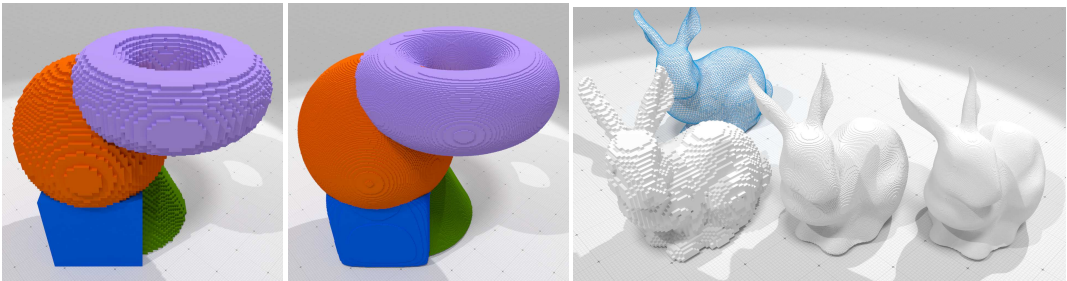


Figure 4: Voxel upscaling using a voxelization of the regularized objects: (left) from 75^3 to 512^3 . (right) Upscaling to 256^3 and 512^3 from the Bunny object in 64^3 and its regularized surface (in blue).

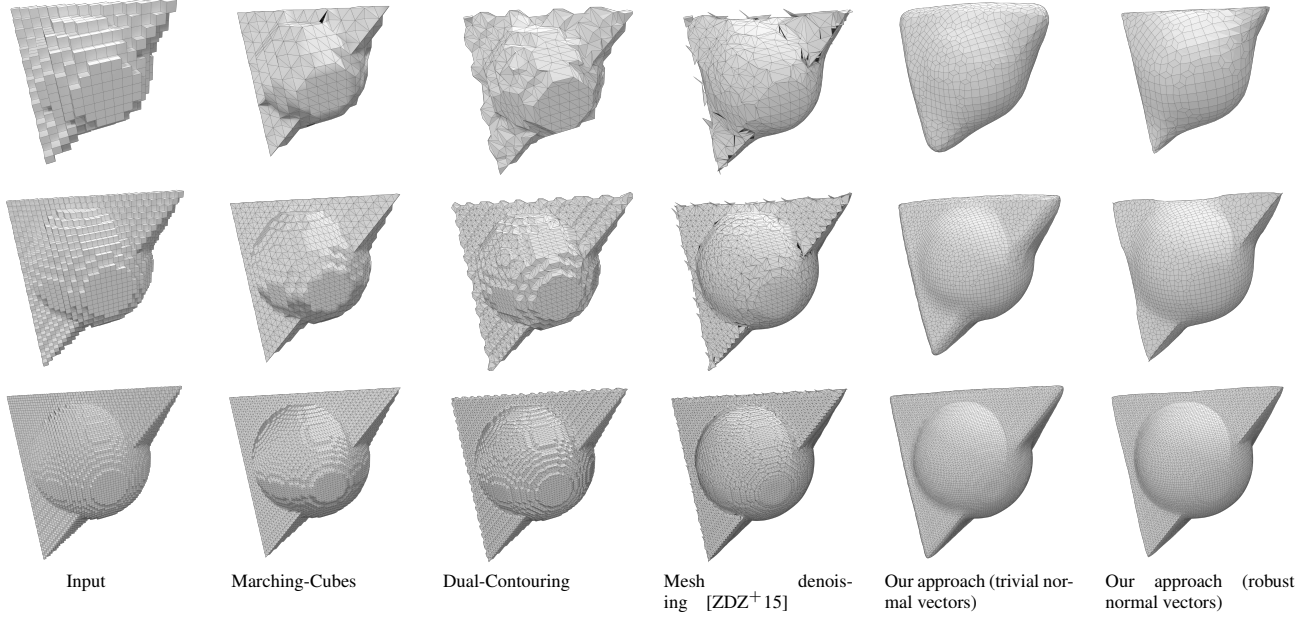


Figure 5: Comparisons on a voxel shape with both sharp and smooth features at three different resolutions: 10^3 , 20^3 and 40^3 . For the last two columns (our results), we have used the same weights for all shapes ($\alpha = 10^{-3}$, $\beta = 1$ and $\gamma = 10^{-1}$).

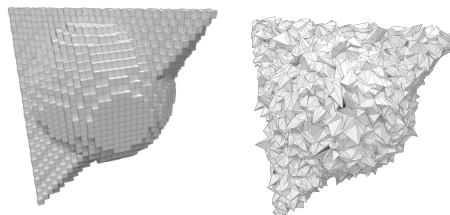


Figure 6: Numerical instability of DC when using a robust normal vector field from [CFGL16] (same as the one in Fig. 8-(d)) but with positions still located in-between adjacent voxels.

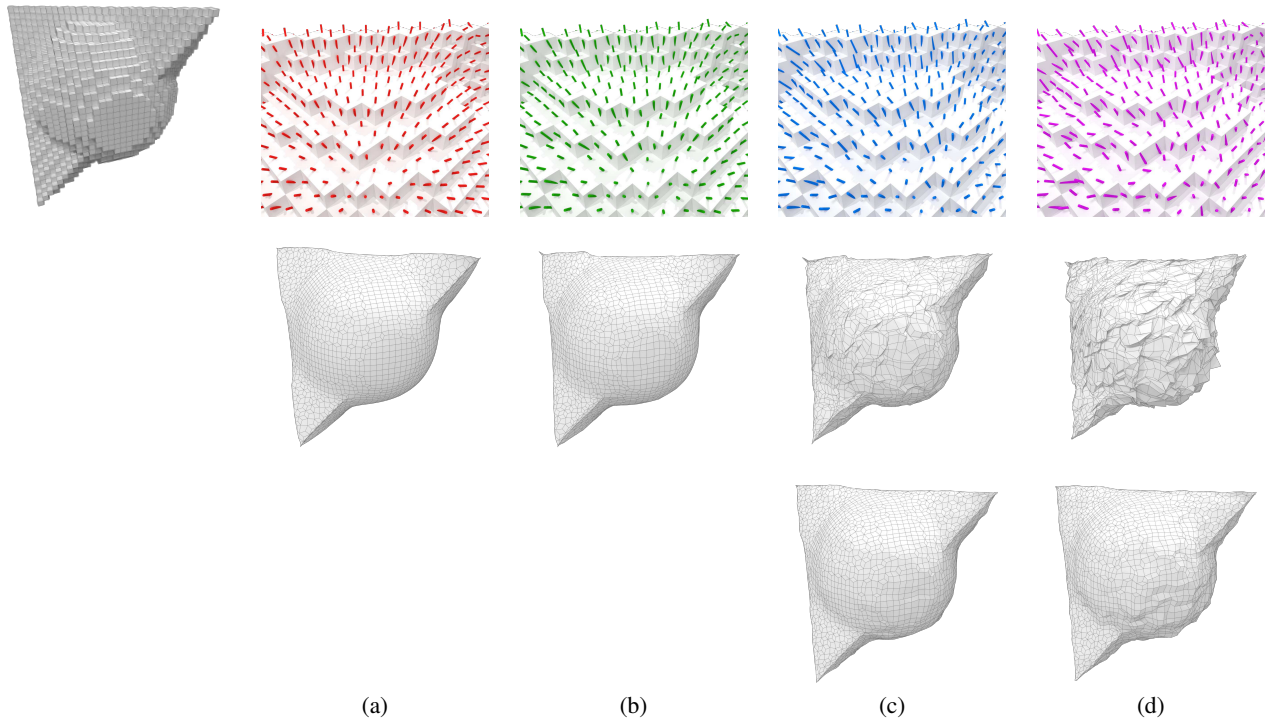


Figure 7: Stability of our method with respect to perturbations in the input normal vector field (40^3 shape, same α , β and γ parameters): (a) the regularization with the input normal vector field from [CFGL16], (b) random shifts ϵ with $\|\epsilon\| < 0.2$ (up to 11°), (c) with $\|\epsilon\| < 0.5$ (up to 26.5°), and (d) with $\|\epsilon\| < 0.8$ (up to 38.7°). For the second row, we have used the default parameters ($\alpha = 10^{-3}$, $\beta = 1$, $\gamma = 10^{-1}$). For the third row, we have reduced the alignment term ($\beta = 10^{-1}$) to handle the strong noise (only for (c) and (d)).

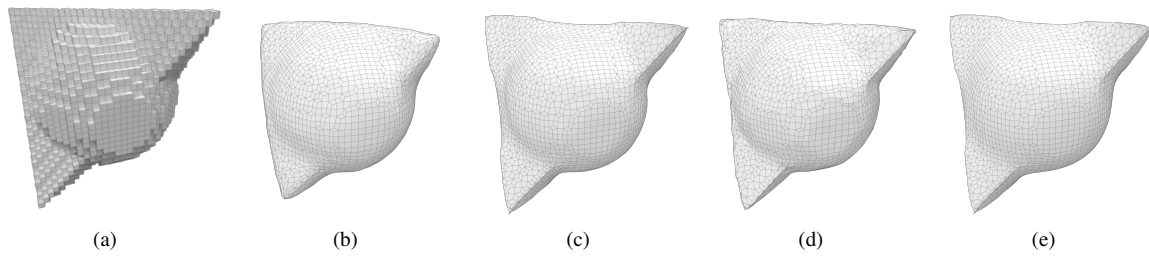


Figure 8: Regularization for various normal vector estimators: (a) trivial normal vectors, (b) isotropic integral invariant estimator [CLL14], (c) robust anisotropic voting based normal vectors [BM12], and (d) piecewise smooth anisotropic normal vectors [CFG16].